Exploration Geophysics (2006) 37, 50-59
Butsuri-Tansa (Vol. 59, No. 1)
Mulli-Tamsa (Vol. 9, No. 1)

Fault reactivation potential during CO_2 injection in the Gippsland Basin, Australia

Peter J. van Ruth [1], Emma J. Nelson [2], Richard R. Hillis [1]

Key Words: Fault reactivation, CO_2 injection, geomechanical risking

ABSTRACT

The risk of fault reactivation in the Gippsland Basin was calculated using the FAST (Fault Analysis Seal Technology) technique, which determines fault reactivation risk by estimating the increase in pore pressure required to cause reactivation within the present-day stress field. The stress regime in the Gippsland Basin is on the boundary between strike-slip and reverse faulting: maximum horizontal stress (~ 40.5 MPa/km) > vertical stress (21 MPa/km) ~ minimum horizontal stress (20 MPa/km). Pore pressure is hydrostatic above the Campanian Volcanics of the Golden Beach Subgroup. The NW-SE maximum horizontal stress orientation (139°N) determined herein is broadly consistent with previous estimates, and verifies a NW-SE maximum horizontal stress orientation in the Gippsland Basin. Fault reactivation risk in the Gippsland Basin was calculated using two fault strength scenarios; cohesionless faults ($C = 0$; $\mu = 0.65$) and healed faults ($C = 5.4$; $\mu = 0.78$). The orientations of faults with relatively high and relatively low reactivation potential are almost identical for healed and cohesionless fault strength scenarios. High-angle faults striking NE-SW are unlikely to reactivate in the current stress regime. High-angle faults oriented SSE-NNW and ENE-WSW have the highest fault reactivation risk. Additionally, low-angle faults (thrust faults) striking NE-SW have a relatively high risk of reactivation. The highest reactivation risk for optimally oriented faults corresponds to an estimated pore pressure increase (Delta-P) of 3.8 MPa (~548 psi) for cohesionless faults and 15.6 MPa (~2262 psi) for healed faults. The absolute values of pore pressure increase obtained from fault reactivation analysis presented in this paper are subject to large errors because of uncertainties in the geomechanical model (in situ stress and rock strength data). In particular, the maximum horizontal stress magnitude and fault strength data are poorly constrained. Therefore, fault reactivation analysis cannot be used to directly measure the maximum allowable pore pressure increase within a reservoir. We argue that fault reactivation analysis of this type can only be used for assessing the relative risk of fault reactivation and not to determine the maximum allowable pore pressure increase a fault can withstand prior to reactivation.

[1] *Cooperative Research Centre for Greenhouse Gas Technologies*
Australian School of Petroleum
The University of Adelaide
North Terrace Campus
South Australia, 5005
Phone: +61 8 8303 6949
Facsimile: +61 8 8030 4345
Email: pvanruth@asp.adelaide.edu.au

[2] *The University of Adelaide*
North Terrace Campus
South Australia, 5005

Manuscript received 9 December, 2004.
Revised manuscript received 23 December, 2005.

INTRODUCTION

The geological storage of carbon dioxide (CO_2) has been proposed as a potential method of reducing greenhouse gas emissions. Subsurface injection of CO_2 at pressures that exceed prevailing formation pressures may potentially reactivate pre-existing faults and generate new faults (Streit and Hillis, 2004). Such brittle deformation can increase fault and fracture permeability, and may lead to the unwanted movement of CO_2 out of the primary storage area (Sibson 1996; Mildren et al., 2002; Streit and Hillis, 2004). Estimates of the fluid pressures that may induce fault slip on faults at a potential injection site can be obtained from geomechanical analysis, e.g., the Fault Analysis Seal Technology (FAST) technique (Mildren et al., 2002). Such analysis requires the knowledge of the geomechanical model (in situ stresses and rock strength data) and the fault orientations.

Fault reactivation analysis can be used to identify whether a fault is oriented to reactivate in the current stress field. Faults identified as optimally oriented in the present-day stress field are at greatest risk of reactivation. Furthermore, the orientation of fractures within the in situ stress field may control whether those fractures act as conduits or barriers to fluid flow (Barton et al., 1998). However, the risk of reactivation of an optimally oriented fault during CO_2 injection can be reduced by minimising the pore pressure increase at the fault, and by appropriate monitoring.

Large uncertainties typically exist in the geomechanical model. In particular, the strength of faults is poorly understood and difficult to measure. It is critical to understand the limitations of the geomechanical model before applying fault reactivation analysis to CO_2 storage projects.

In this paper, the application of geomechanical fault reactivation analysis to a potential CO_2 storage site – the offshore Gippsland Basin – is considered. The geomechanical model (in situ stresses and rock strength data) is constrained, and fault reactivation analysis for two assumed fault strength scenarios is presented. The results of the fault reactivation analysis are shown to be dependent on uncertainties in the geomechanical model.

Gippsland Basin

The Gippsland Basin is located in the south-eastern corner of Australia (Figure 1). The offshore Gippsland Basin is one area being studied as a potential CO_2 storage site within Australia (Root et al., 2004; Gibson-Poole et al., 2006). The study area within the offshore Gippsland Basin is bounded to the north and south by E-W trending fault systems separating it from the Northern Terrace and the Southern Terrace respectively (Figure 1). Potential CO_2 injection horizons in the Gippsland Basin include sandstone units within the Latrobe Group (Figure 2). The Gurnard Formation, at the top of the Latrobe Group, may provide a sealing unit. However, the Lakes Entrance Formation is considered herein to be the primary seal to the Latrobe Group reservoirs in the context of CO_2 storage (Gibson-Poole et al., 2006). Many faults mapped within the Latrobe Group appear to terminate within the Latrobe

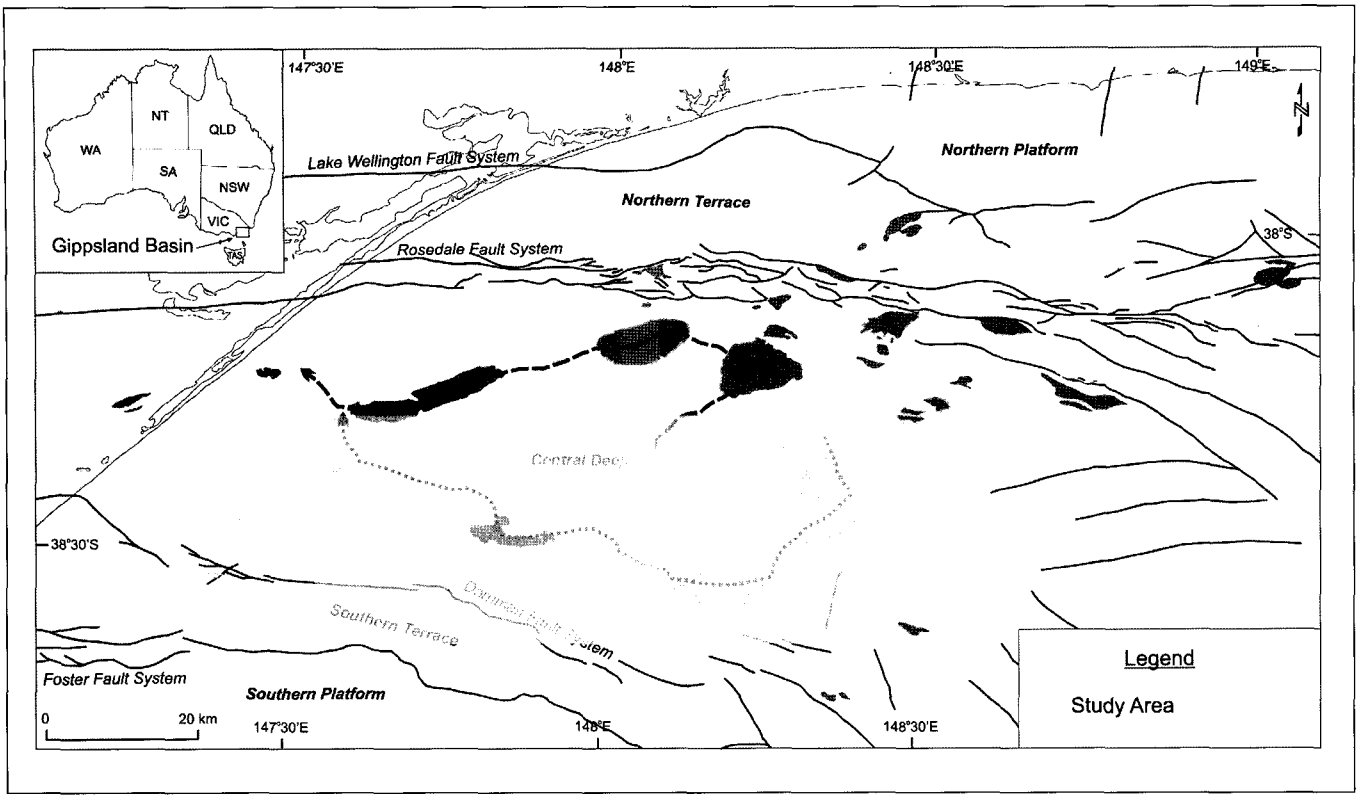

Fig. 1. Study location map. Modified after Power et al. (2001).

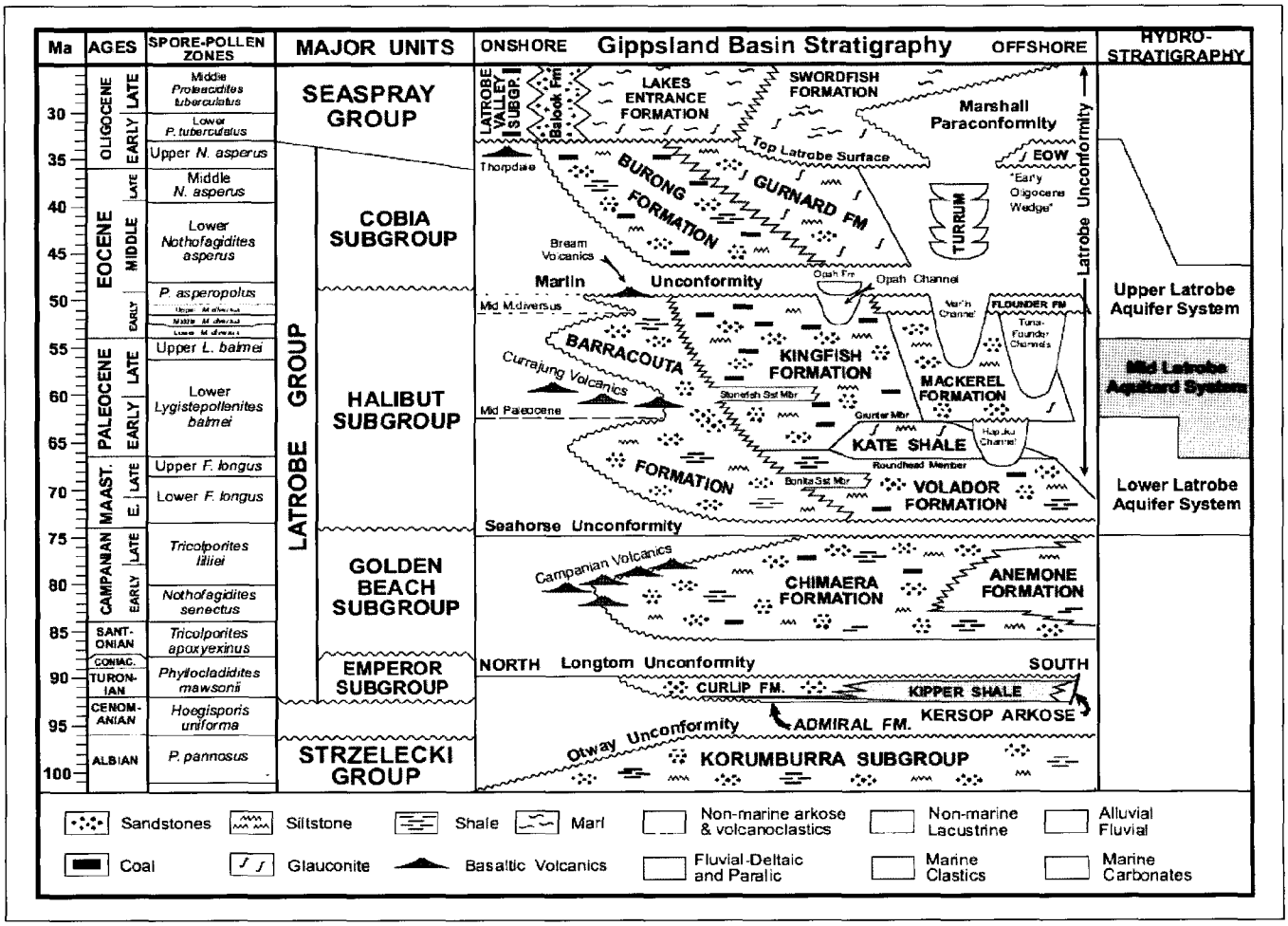

Fig. 2. Stratigraphic table for the offshore Gippsland Basin (modified after Bernecker and Partridge, 2001; Root et al., 2004).

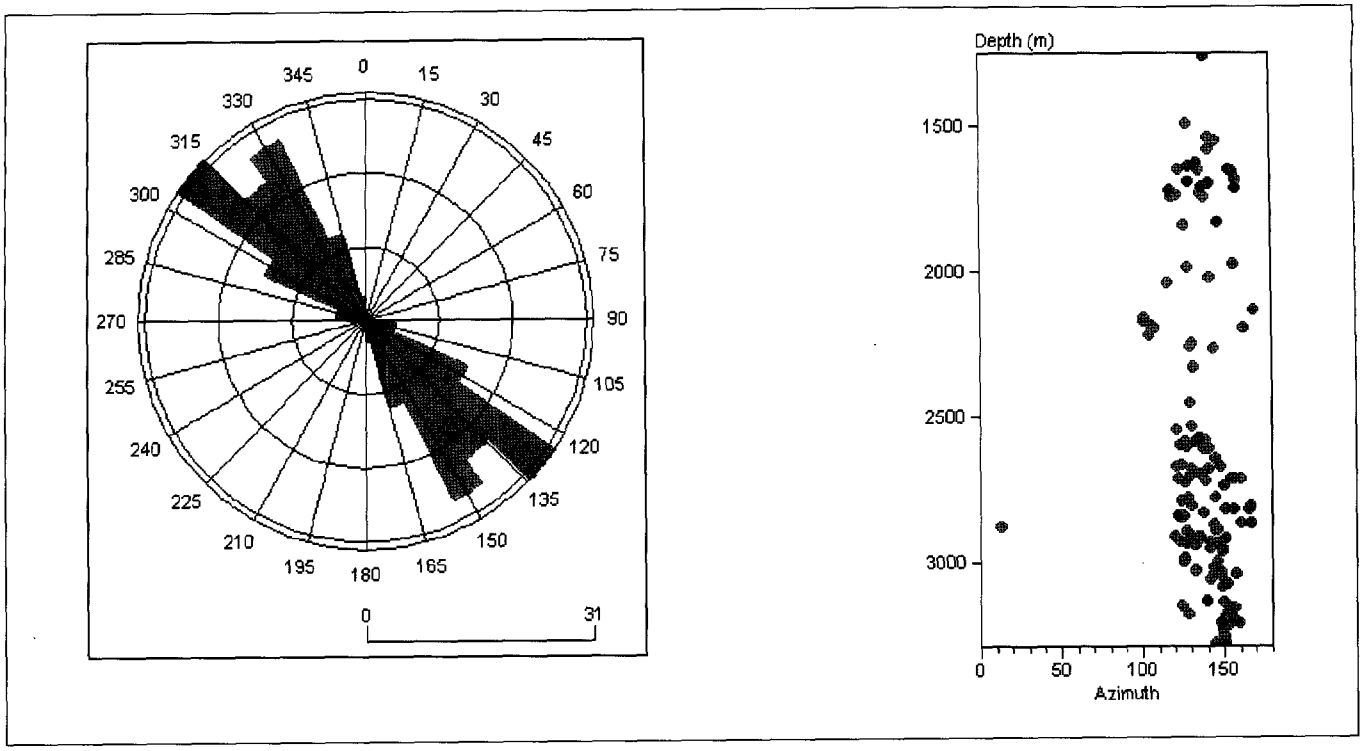

Fig. 3. Maximum horizontal stress orientation, Gippsland Basin. From borehole breakouts (shown in red): mean = 139°, standard deviation = 15°, count = 118. From drilling induced tensile fracture (shown in blue): mean = 140°, standard deviation = 11.5°, count = 16.

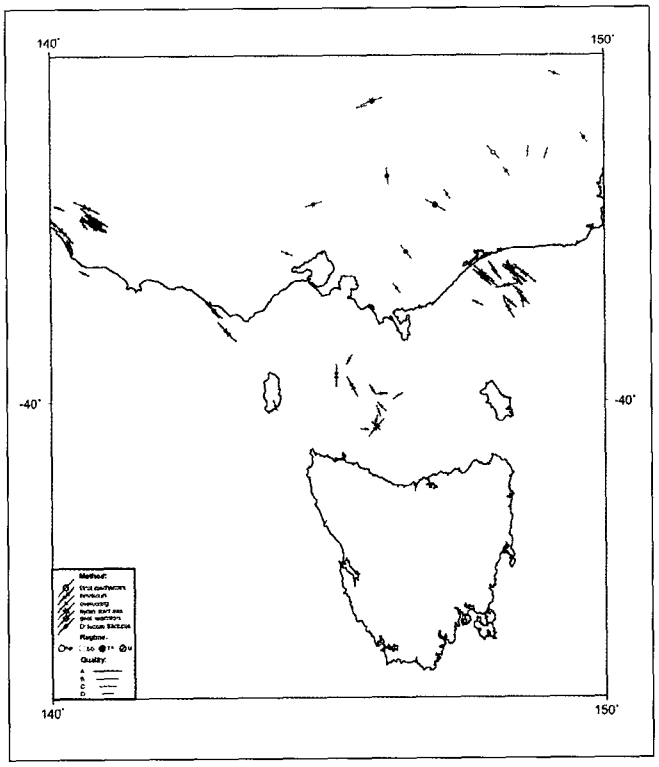

Fig. 4. Maximum horizontal stress orientation in South Eastern Australia (after Hillis et al., 1998).

Group, and therefore are unlikely present a containment risk to any CO_2 storage project. However, some faults appear to cut the Top Latrobe Unconformity, and may present a containment risk if they lie within the migration pathway of an injected CO_2 plume (Root et al., 2004).

GEOMECHANICAL MODEL

The strength of the fault plane and the in situ stress tensor must be constrained to undertake fault reactivation analysis. The geomechanical model consists of in situ stress and rock strength data. The geomechanical model provides the basis for all geomechanical studies and the accuracy of a geomechanical study is dependent on the accuracy of the geomechanical model data. The Gippsland Basin geomechanical model is outlined in the following section.

Maximum Horizontal Stress Orientation

The orientation of maximum horizontal stress can be measured from the occurrence of borehole deformation. Borehole breakouts and drilling-induced tensile fractures (DITFs) form at a particular angle to the in situ stresses. Therefore, the orientation of the stresses can be inferred from the orientation of any breakouts or DITFs in a borehole.

Intervals of borehole breakouts and drilling-induced tensile fractures in the Gippsland Basin have been identified from image logs (Nelson and Hillis, 2005). The average S_{Hmax} orientation derived from the occurrence of borehole breakouts is 139°N (standard deviation = 15°) (Table 1; Figure 3). The average maximum horizontal stress orientation derived from axial DITF occurrence is 140°N (standard deviation = 11.5°) (Table 2; Figure 3). The horizontal stress orientation determined from DITFs in the region is highly consistent with the S_{Hmax} azimuth derived from borehole breakouts.

WELL	Mean S_{hmax} Orientation (°N)	Standard Deviation	Count	Quality
BEARDIE 1	143.17	10.49	3	D
BLACKBACK 3	169.53	11.69	5	C
EAST PILCHARD 1	137.48	10.84	26	A
LONGTOM 1	103.6	2.33	5	C
MOONFISH 1ST1	148.25	12.14	8	B
WEST TUNA 8	147.78	8.82	20	A
WEST TUNA 32	126.25	2.86	4	D
WEST TUNA 37	146.56	5.96	19	A
WEST TUNA 39	132.51	10.142	11	A
WEST TUNA 44	125.76	3.098	17	A

Table 1. Maximum horizontal stress orientation within the Gippsland Basin derived from borehole breakouts.

WELL	Mean S_{hmax} Orientation (°N)	Standard Deviation	Count	Quality
BEARDIE 1	131.38	7.33	6	B
EAST PILCHARD 1	128.5	6.53	2	D
LONGTOM 1	139	0	1	D
MOONFISH 1ST1	153.76	4.15	4	D
WEST TUNA 8	145.35	4.50	3	D

Table 2. Maximum horizontal stress orientation within the Gippsland Basin derived from drilling-induced tensile fractures.

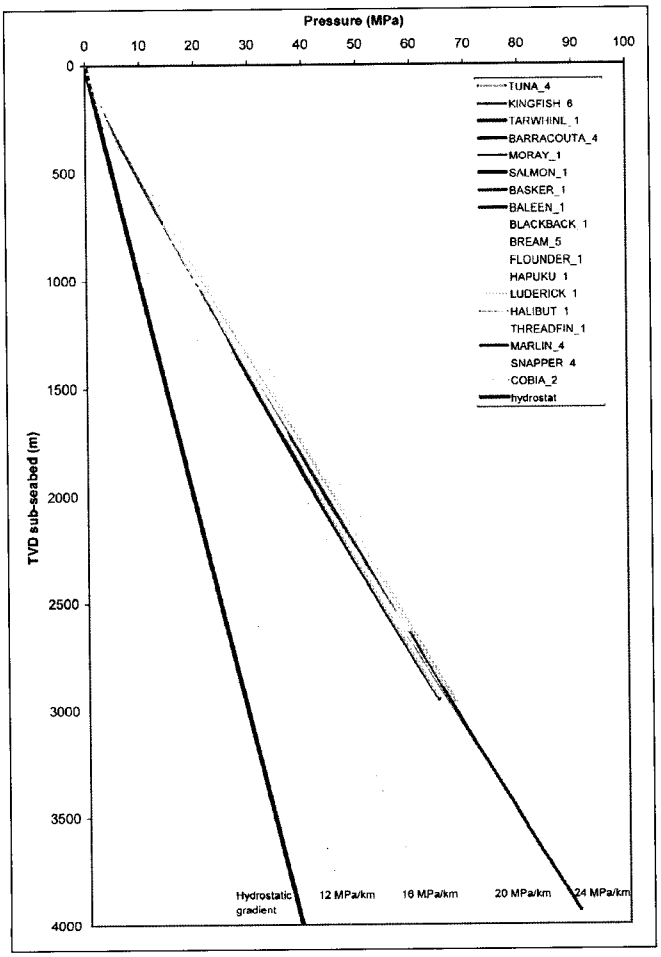

Fig. 5. Vertical stress estimates in the Gippsland Basin. Depth is relative to sea floor.

Locality	S_{Hmax} Azimuth (°N)
FLOUNDERS	122
HAPUKU-1	135
FORTESCUE-1	80
WHITING-2	127
SELENE-1	123
OMEO-1	113
HERMES-1	130
HELIOS-1	151
WIRRAH-3	138
WIRRAH-1	131

Table 3: Previously calculated maximum horizontal stress orientations within the Gippsland Basin (Hillis et al., 1998).

Previous estimates of maximum horizontal stress (S_{Hmax}) orientation were based on logs from 4-arm dipmeter tools at ten locations within the Gippsland Basin (Hillis et al., 1998). The average maximum horizontal stress orientation based on previous data is 125°N (Table 3; Figure 4). Breakout interpretation from 4-arm dipmeter logs is less reliable than image log interpretation, as evidenced in the scatter of orientations listed in Table 3 (Brudy and Kjorholt, 2001). The dipmeter logs were not available for this study and therefore the quality of the interpretation could not be assessed. The orientation of S_{Hmax} determined in the West Tuna area herein is consistent within the wells studied and is considered more reliable than the existing data. The S_{Hmax} orientation of 139°N determined herein is broadly consistent with the orientation calculated previously and verifies a NW-SE maximum horizontal stress orientation in the Gippsland Basin.

Well	Date	Depth TVDSS (M)	Test Type	Pressure (MPa)
Amberjack_1	May-90	1000.00	LOT	16.37
Drummer_1	October-85	805.50	LOT	21.26
Kipper_1	March-86	830.00	LOT	19.73
West Tuna_39	July-97	2154.00	LOT	20.31
Anemone_1	July-89	1078	REP_LOT	26.83
Anemone_1	July-89	3041	REP_LOT	53.22
Athene_1	June-83	507	REP_LOT	6.49
Athene_1	June-83	1170	REP_LOT	19.93
Baleen_1	November-81	200.05	REP_LOT	3.39
Baleen_1	November-81	556.55	REP_LOT	10.80
Basker_1	September-83	473	REP_LOT	7.18
Basker_Sth1	December-83	675	REP_LOT	10.05
Blackback_1	March-89	1225	REP_LOT	20.57
Devilfish_1	May-90	1060.2	REP_LOT	20.41
East Halibut_1	September-85	802	REP_LOT	16.48
Grunter_1	November-84	834	REP_LOT	15.18
Grunter_1	November-84	3528	REP_LOT	80.37
Gummy_1	June-90	528.6	REP_LOT	6.84
Gummy_1	June-90	1165.6	REP_LOT	18.73
Helios_1	October-82	318	REP_LOT	3.70
Helios_1	October-82	1155.6	REP_LOT	20.08
Helios_1	October-82	2972	REP_LOT	50.61
Leatherjacket_1	March-86	605	REP_LOT	10.80
Luderick_1	July-83	771	REP_LOT	15.21
Moonfish_2	December-94	803.2	REP_LOT	12.73
Mulloway_1	February-89	740	REP_LOT	12.34
Perch_2	March-85	779	REP_LOT	14.82
Pilotfish_1	December-82	917	REP_LOT	17.34
Selene_1	February-82	1241	REP_LOT	25.94
Snapper_4	July-83	1480	REP_LOT	28.85
Terakihi_1	April-90	1103	REP_LOT	20.73
Tuna_4	August-84	773	REP_LOT	16.70
Tuna_4	August-84	2413	REP_LOT	47.58
Tuna_4	August-84	3198	REP_LOT	62.72
Veilfin_1	April-84	794	REP_LOT	15.10
Loy_Yang_1		254.1	REP_LOT	5.19
Wrixondale_1		275.8	REP_LOT	6.19

Table 4. Leak-off tests in the Gippsland Basin. REP LOT refers to leak-off tests recorded in well completion reports but where no pressure decline plot is available.

Vertical Stress

Vertical stress (σ_v) is the stress applied at any given point due to the weight of the overlying rock mass and fluids. Vertical stress magnitude can be estimated by integrating the bulk density of the overlying rock mass and fluids with depth (e.g., Engelder, 1993):

$$\sigma_V = \int_z^0 \rho(z) g\, dz \qquad (1)$$

where g is the gravitational acceleration (9.81 m/s^2), z is depth and ρ is the density of the rocks and fluids.

Wireline density log measurements, where available, are used herein to estimate the bulk density of the sediments. Density log measurements were disregarded where the density log correction (e.g., DRHO) was greater than 0.1 t/m^3. Bulk density in the section above the top of the density log was estimated from check-shot log velocities, using an empirical relationship between density and velocity. Vertical stress values obtained for the Gippsland Basin are shown in Figure 5.

Scenario	Depth m	σ_v MPa	σ_H MPa	σ_h MPa	P_P MPa	θ_H orient. °N	C MPa	μ
Faults: healed	2300	48.3	93.2	46.0	22.5	139	5.4	0.78
Faults: cohesionless	2300	48.3	93.2	46.0	22.5	139	0	0.65

Table 5. Geomechanical model data. σ_v is vertical stress, σ_H is maximum horizontal stress, σ_h is minimum horizontal stress, P_P is pore pressure, θ_H orient. is the orientation of the maximum horizontal stress, C is cohesion, and μ is the coefficient of friction.

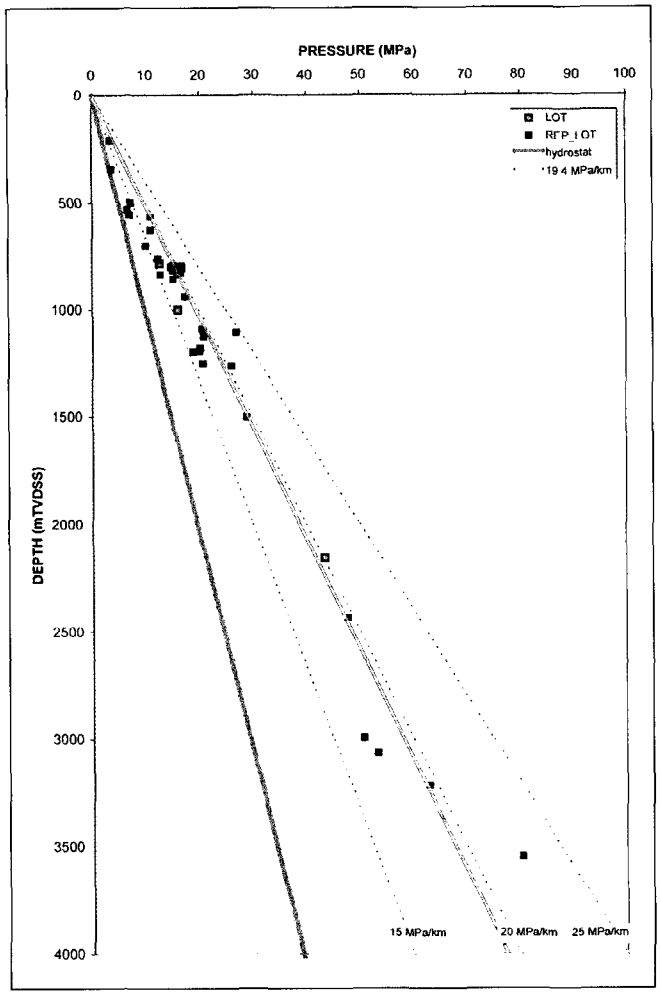

Fig. 6. Minimum horizontal stress magnitude in the Gippsland Basin derived from leak-off tests.

Minimum Horizontal Stress

Minimum horizontal stress (S_{hmin}) magnitude can be estimated from leak-off test (LOT) and mini-fracture test data. While leak-off pressures in vertical wells reflect the horizontal stress, the same pressure tests from deviated wells are a function of the vertical and horizontal stresses and wellbore trajectory with respect to those stresses (Aadnoy, 1990; Brudy and Zoback, 1993). Therefore, only leak-off pressures from vertical wells were used in this study to constrain S_{hmin} in the Gippsland Basin. Leak-off test data from the Gippsland Basin are consistent and indicate S_{hmin} ~20 MPa/km (Table 4; Figure 6). A minimum horizontal stress gradient of ~20 MPa/km is high compared with those reported in other Australian Basins (Hillis et al., 1998). Leak-off pressures from the nearby Otway Basin suggest that the minimum horizontal stress in the Otway Basin is ~16 MPa/km (Hillis et al., 1995).

Maximum Horizontal Stress

Frictional limits

Frictional limits theory states that the ratio of the maximum to minimum effective stress cannot exceed the magnitude required to cause faulting on an optimally oriented, pre-existing, cohesionless fault plane (Sibson, 1974). The frictional limit to stress is given by:

$$\frac{\sigma_1 - P_P}{\sigma_3 - P_P} \leq \left\{\sqrt{(\mu^2 + 1)} + \mu\right\}^2 , \qquad (2)$$

where μ is the coefficient of friction, P_P is the pore pressure, σ_1 is the maximum principal stress, and σ_3 is the minimum principal stress. S_{Hmax} magnitude can be constrained to less than 44.4 MPa/km by substituting the Gippsland stress tensor values (S_{hmin} ~ 20 MPa/km, σ_v ~ 21 MPa/km, P_P ~ 9.8 MPa/km, P_w ~ 11.2 MPa/km) into equation 2 and assuming $\mu = 0.65$.

Observation of drilling-induced tensile fractures

Sixteen sections of DITF were observed in the study area (Figure 3). Pore pressures were normal at the depth of the DITFs and wells were drilled slightly overbalanced (P_w = 11 MPa/km). Substitution of the in situ stress tensor values determined herein (S_{hmin}, P_p and P_w) into Equation 3

$$\sigma_{\theta\theta\,min} = 3S_{h\,min} - S_{H\,min} - P_w - P_p \leq 0 , \qquad (3)$$

where P_w is the static mud weight, and $\sigma_{\theta\theta\,min}$ is the minimum circumferential stress, indicates that the magnitude of S_{Hmax} in the Gippsland Basin is ~39 MPa/km. The S_{Hmax} magnitude calculated using equation 2 may be a lower bound to S_{Hmax}, because the DITFs, particularly in Moonfish, Beardie, West Tuna-8, and East Pilchard-1 are well developed and it is likely that the tensile strength of the West Tuna rocks (which are consolidated and cemented) is greater than zero.

Observation of transverse drilling-induced tensile fractures

Elasticity theory predicts formation of both transverse and axial drilling-induced tensile fractures (DITFs) in vertical wells depending on the magnitude of the principal in situ stresses, pore-pressure, and mud weight. Drilling-induced tensile fractures initiate in very specific stress environments. A lower bound to the maximum horizontal stress (S_{Hmax}) magnitude can be constrained from the occurrence of axial DITFs provided the minimum horizontal (S_{hmin}) stress is known. The occurrence of transverse DITFs can be used to constrain a lower bound to maximum and minimum horizontal stress magnitudes (Nelson et al., 2005). The stress field can be constrained to one on the border of strike-slip and reverse faulting ($S_{Hmax} > S_{hmin} > \sigma_v$), without requiring knowledge of the S_{hmin} or S_{Hmax} magnitude, from the observation of transverse DITFs on image logs (Nelson et al., 2005). The observation of

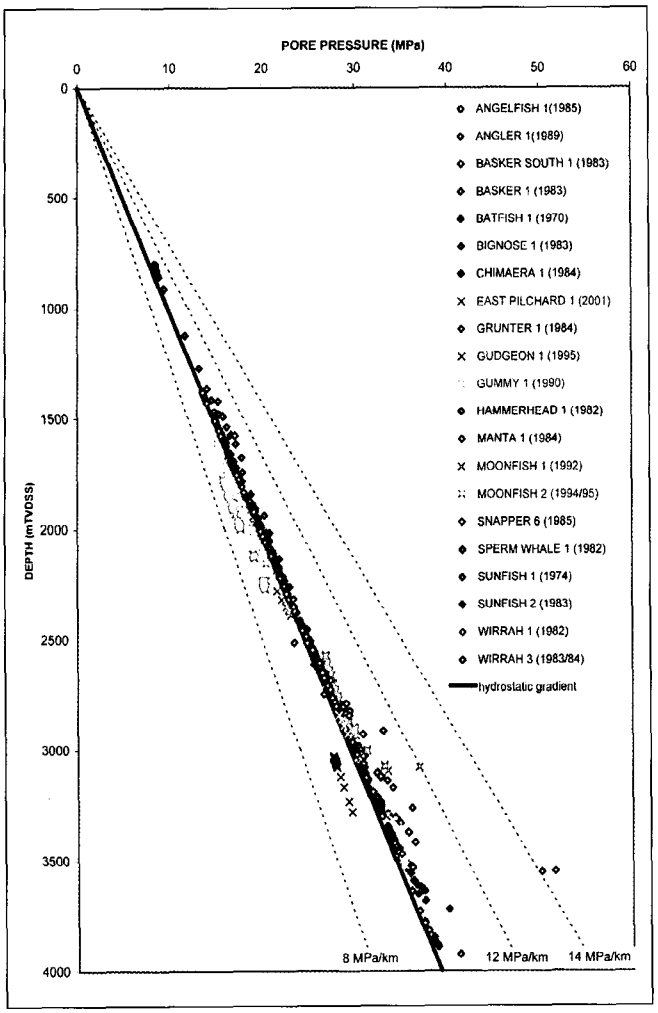

Fig. 7. Pore pressure derived from wireline formation tests in the Gippsland Basin. There is no overpressure above the Campanian Volcanics of the Golden Beach Subgroup.

transverse DITFs in the Gippsland Basin wells West Tuna-8, West Tuna-39, Moonfish-ST1, and Blackback-3 (Nelson et al., 2005), combined with wireline log data, leak-off tests and pore pressure data, constrain the in situ stress tensor at the depth of observation to the border between a strike-slip and a reverse faulting regime, where $S_{Hmax} \sim 40.5$ MPa/km $> S_{hmin} \sim \sigma_v = 20$ MPa/km. Readers are directed to Nelson et al. (2005) and references therein for a more detailed description of the methodology.

Maximum horizontal stress estimates from frictional limits, axial DITFs, and transverse DITFs are consistent, and suggest a S_{Hmax} of ~40.5 MPa/km. Therefore, the stress regime in the Gippsland Basin is on the boundary between strike-slip and reverse faulting. A strike-slip stress regime where maximum horizontal stress (~40.5 MPa/km) > vertical stress (21 MPa/km) ~ minimum horizontal stress (20 MPa/km) is used herein (Table 5). The in situ stress estimates presented herein are consistent with previous estimates of in situ stress in the Gippsland Basin (Nelson et al., 2005; Nelson and Hillis, 2005).

Pore Pressure

Pore pressures were determined from wireline formation tests in 21 Gippsland wells (Figure 7). The pore pressure gradient in the West Tuna area is generally hydrostatic, with no overpressure above 2800 m TVDSS (Figure 7). Overpressure at 2800 m coincides with the depth of the Campanian Volcanics of the Golden Beach Subgroup. The East Pilchard, Angelfish, Gummy, Bignose, Snapper 6, and Manta wells are overpressured below the volcanics. None of the LOT pressures were from overpressured intervals and no post production pore pressure measurements are available. Therefore, the effects of pore pressure depletion and the reservoir stress path (e.g., Teufel et al., 1991; Santarelli et al., 1998) have not been analysed in this study. Virgin pore pressure conditions have been assumed in this study.

Fault Strength

Reliable fault strength data is required to undertake geomechanical fault reactivation analysis. Frictional sliding and sample loading experiments give the most reliable rock strength

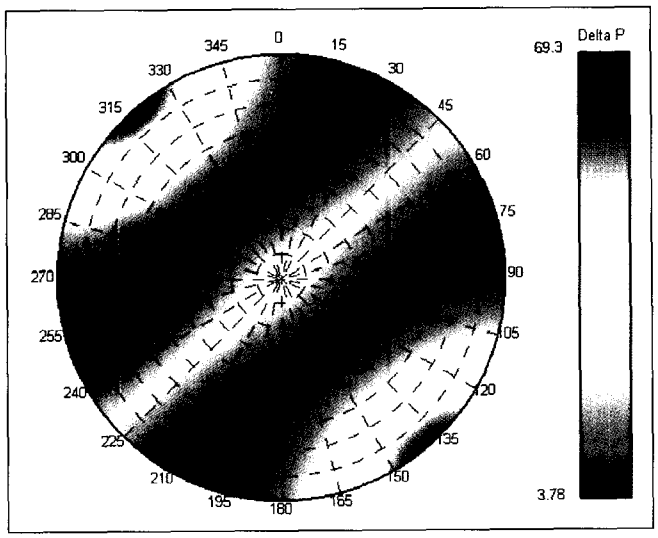

Fig. 8. Stereonet showing the reactivation risk for cohesionless faults at 2300 m depth in the Gippsland Basin. Faults orientations are plotted as poles to planes and have been coloured according to estimated maximum sustainable pore pressure increase (Delta-P). Delta-P is in megaPascals. The maximum risk (for optimally oriented faults) corresponds to a fault reactivation risk of 3.8 MPa (~548 psi).

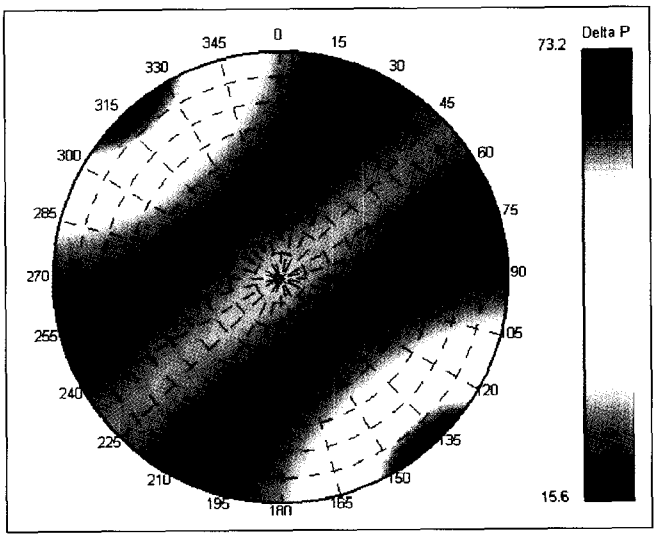

Fig. 9. Stereonet showing the reactivation risk for healed faults at 2300 m depth in the Gippsland Basin. Faults orientations are plotted as poles to planes and have been coloured according to estimated maximum sustainable pore pressure increase (Delta-P). Delta-P is in megaPascals. The maximum risk (for optimally oriented faults) corresponds to a fault reactivation risk of 15.6 MPa (~2262 psi).

data. The coefficient of friction for cohesionless faults obtained from frictional sliding experiments typically ranges between 0.60 and 0.85 (Handin, 1963; Byerlee, 1978; Shimamoto and Logan, 1981). Several fault reactivation studies (e.g., Barton el al., 1995; Barton et al., 1998; Wiprut and Zoback, 2000) assume that faults are cohesionless and behave according to a Byerlee (1978) type friction law. However, frictional sliding experiments do not take into account fault cohesion which may form as a result of lithification of a fault (Dewhurst et al., 2002). Laboratory loading experiments on intact fault rock show that such healed fault rock can have considerable cohesion and, in some cases, is stronger than the host rock (Dewhurst and Jones, 2002; Dewhurst et al., 2002). It is likely that strength of faults in the subsurface varies widely, depending on factors such as the faulted material, fault rock material, and age of faulting. Sample loading and frictional loading experiments are rarely undertaken. Rock strength can be empirically determined from wireline log data. However, wireline log measurements give bulk rock properties that may not be analogous to fault strength. Hence, it may not be possible to derive fault, as opposed to intact rock, strength data from wireline log data. Furthermore, log-derived fault strength values should be calibrated using laboratory-derived strength data, which are rarely available.

Fault strength data for the Gippsland Basin were not available for this study. Two fault strength scenarios were considered; healed faults and cohesionless faults. Healed faults were assumed to have the same fault strength as a cataclasite from the Pretty Hill Formation in the nearby Otway Basin tested by Dewhurst and Jones (2002). Cohesionless faults were considered to have a coefficient of friction of 0.65, which is consistent with assumptions made to constrain the maximum horizontal stress magnitude (Nelson et al., 2005). Both fault strength scenarios are considered to fall within the range of possible fault strengths in the Gippsland Basin.

FAULT REACTIVATION ANALYSIS

The injection of CO_2 into the subsurface may result in an increase in the reservoir pore pressure. Increasing pore pressure can lead to the brittle failure of rocks, which occurs when the stress acting on a rock exceeds rock strength (e.g., Sibson, 1996; Mildren et al., 2002).

The relative risk of fault reactivation, based on fault orientation within the in situ stress field, can be estimated from geomechanical risking. The relative risk of fault reactivation was calculated herein using the FAST (Fault Analysis Seal Technology) technique, which determines fault reactivation risk by estimating the theoretical increase in pore pressure required to cause reactivation (Mildren et al., 2002). Readers are directed to Mildren et al. (2002), Streit and Hillis (2004), and references therein for further information.

The geomechanical model data used to calculate fault reactivation risk is summarized in Table 5. The maximum sustainable pore pressure increase for cohesionless faults for all fault orientations in the Gippsland Basin at 2300 m is shown in Figure 8 on a stereonet. High-angle faults striking NE-SW are unlikely to reactivate in the current stress regime (cool colours in Figure 8). High-angle faults oriented SSE-NNW and ENE-WSW have the highest fault reactivation risk (hot colours in Figure 8). Additionally, low-angle faults (thrust faults) striking NE-SW have a relatively high risk of reactivation. The highest reactivation risk for optimally oriented cohesionless faults was estimated to be 3.8 MPa (~548 psi). The maximum sustainable pore pressure for healed faults is shown in Figure 9. The highest reactivation risk for optimally oriented healed faults was estimated to be 15.6 MPa (~2262 psi) (Figure 9). These results are broadly consistent with those of Root et al. (2004), who analysed relative fault reactivation for nine faults within the Gippsland Basin using the slip-tendency method.

DISCUSSION

Two fault strength scenarios were used to calculate fault reactivation risk; cohesionless faults and healed faults. Fault orientations with high and low reactivation risks are similar for healed and cohesionless faults (Figures 8 and 9). Therefore, fault reactivation analysis of the type presented herein can be used to determine the relative risk of fault reactivation in the in situ stress field. However, the absolute values of fault reactivation risk for cohesionless faults were significantly less than for healed faults. The highest reactivation risk (for optimally oriented faults) was estimated to be a 3.8 MPa (~548 psi) increase in pore pressure for cohesionless faults and a 15.6 MPa (~2262 psi) increase in pore pressure for healed faults. Therefore, the lack of reliable fault strength data in the Gippsland Basin results in large uncertainties in modelled fault reactivation risks (Delta-P). Furthermore, maximum horizontal stress was constrained, in part, by assuming that optimally oriented cohesionless faults exist within the study area. Hence, estimates of the maximum horizontal stress and fault reactivation risk (Delta P) presented herein are not completely independent of each other. Therefore, the results of the fault reactivation analysis presented herein should only be used for assessing relative risk of fault reactivation.

The increase in pore pressure during CO_2 injection will depend, in part, on factors including injection volume, injection rate, the size of the injection interval, and the permeability distribution within the target reservoir. The larger the increases in reservoir pore pressure at a fault, the greater the probability that the fault will reactivate. Therefore, an injection scenario which minimises the reservoir pore pressure increase near all known faults should be chosen.

Reactivation risk for faults which do not appear to extend through the seal may not be a containment risk. However, reactivation of such faults is undesirable because:

- Increase fault zone permeability may lead to unexpected / unwanted fluid movement within the Latrobe Unconformity;
- These faults appear to terminate within the Latrobe Group. However, they may extend to cut the Top Latrobe Unconformity beneath seismic resolution;
- These faults may cut the Top Latrobe Unconformity should significant displacement of the faults occur during reactivation;
- These faults may form part of a larger fault and fracture permeability network, and;
- Reactivation of these faults may cause unwanted subsidence.

As such, an injection scenario that minimises pore pressure increase at all known faults is advised for any potential CO_2 storage project within the Gippsland Basin.

CONCLUSIONS

The stress regime in the Gippsland Basin is on the boundary between strike-slip and reverse faulting: maximum horizontal stress (~ 40.5 MPa/km) > vertical stress (21 MPa/km) ~ minimum horizontal stress (20 MPa/km). Pore pressure is hydrostatic above the Campanian Volcanics of the Golden Beach Subgroup. The maximum horizontal stress orientation (139°N) determined herein verifies a NW-SE maximum horizontal stress orientation in the Gippsland Basin.

Subsurface injection of CO_2 at excessive pressure may lead to fault reactivation. Geomechanical information on sub-surface stresses and rock strength can be used to assess the relative risk of reactivation of individual faults. Fault reactivation risk in the Gippsland Basin was calculated using two fault strength scenarios; cohesionless faults ($C = 0$; $\mu = 0.65$) and healed faults ($C = 5.4$; $\mu = 0.78$). The orientations of faults with relatively high and relatively low reactivation potential are almost identical for healed and cohesionless fault strength scenarios. High-angle faults striking NE-SW are unlikely to reactivate in the current stress regime. High-angle faults oriented SSE-NNW and ENE-WSW have the highest fault reactivation risk. Additionally, low-angle faults (thrust faults) striking NE-SW have a relatively high risk of reactivation. The highest reactivation risk for optimally oriented faults corresponds to an estimated pore pressure increase (Delta-P) of 3.8 MPa (~548 psi) for cohesionless faults and 15.6 MPa (~2262 psi) for healed faults. However, large uncertainties in the geomechanical model may exist, leading to large errors in calculated pore pressure increase required to cause fault reactivation. Therefore, fault reactivation analysis of this type should only be used to identify the relative risk of fault reactivation in the present-day stress field, and not to determine the maximum allowable pore pressure increase a fault can withstand without reactivation during CO_2 injection.

REFERENCES

Aadnoy, B.S., 1990, Inversion technique to determine the in situ stress field from fracturing data: *Journal of Petroleum Science and Engineering*, **4**, 127–141.

Barton, C.A., Zoback, M.D., and Moos, D., 1995, Fluid flow along potentially active faults in crystalline rock: *Geology*, **23**, 683–686.

Barton, C., Hickman, S., Morin, R., Zoback, M. and D. Benoit, 1998, *Reservoir-scale Fracture Permeability in the Dixie Valley, Nevada, Geothermal Field*: SPE/ISRM 47371.

Bernecker, T. and Partridge, A.D., 2001, Emperor and Golden Beach Subgroups: the onset of Late Cretaceous sedimentation in the Gippsland Basin, SE Australia. In: Hill, K.C., and Bernecker, T. (eds), *Eastern Australasian Basins Symposium: a refocused energy perspective for the future*: Petroleum Exploration Society of Australia, 391–402.

Brudy, M., and Kjorholt, H., 2001, Stress orientation on the Norwegian continental shelf derived from borehole failures observed in high-resolution borehole imaging logs: *Tectonophysics*, **337**, 65–84.

Brudy, M., and Zoback, M.D.,1993, Compressive and tensile failure of boreholes arbitrarily inclined to principal stress axes: Application to the KTB boreholes, Germany: *International Journal of Rock Mechanics and Mining Science*, **30**, 1035–1038.

Byerlee, J.D., 1978, Friction of Rocks, *Pure and Applied Geophysics*, **116**, 615–626.

Dewhurst, D.N., and Jones, R.M., 2002, Geomechanical, microstructural and petrophysical evolution in experimentally re-activated cataclasites: application to fault seal prediction: *AAPG Bulletin*, **86**, 1383–1405.

Dewhurst, D.N., Jones R.M., Hillis, R.R., and Mildren, S.D., 2002, Microstructural and Geomechanical Characterisation of Fault Rocks from the Carnarvon and Otway Basins: *APPEA Journal*, **42**, 167–186.

Engelder, T., 1993, *Stress Regimes in the Lithosphere*: Princeton University Press, 457pp.

Gibson-Poole, C.M., Svendsen, L., Underschultz, J., Watson, M.N., Ennis-King, J., van Ruth, P., Nelson, E., Daniel, R.F., and Cinar, Y., 2006, Gippsland Basin Geosequestration, Potential Solution for the Latrobe Valley Brown Coal CO_2 emissions: *APPEA Journal*, **46**, (in press).

Handin, J., Hager, R.V.Jr., Friedman, M., and Feather, J.N., 1963, Experimental deformation of sedimentary rocks under confining pressure: pore pressure tests: *AAPG Bulletin*, **47**, 718–755.

Hillis, R.R., Meyer, J.J., and Reynolds, S.D., 1998, The Australian stress map: *Exploration Geophysics*, **29**, 420–427.

Hillis, R.R., Monte, S.A., Tan, C.P., and Willoughby, D.R., 1995, The contemporary stress field of the Otway Basin, South Australia: Implications for hydrocarbon exploration and production: *APEA Journal*, 494–506.

Mildren, S.D., Hillis, R.R., and Kaldi, J., 2002, Calibrating predictions of fault seal reactivation in the Timor Sea: *APPEA Journal*, **42**, 187–202.

Nelson, E.J., Meyer, J.J., Hillis R.R., and Mildren, S.D., 2005, Transverse drilling-induced tensile fractures in the West Tuna area, Gippsland Basin, Australia: implications for the in situ stress regime: *International Journal of Rock Mechanics and Mining Sciences*, **42**, 361–371.

Nelson, E.J., and Hillis, R.R., 2005, In Situ stresses of the West Tuna area, Gippsland Basin: *Australian Journal of Earth Sciences*, **52**, 299–313.

Power, M.R., Hill, K.C., Hoffman, N., Bernecker, T., and Norvick, M., 2001, The structural and tectonic evolution of the Gippsland Basin: results from 2D section balancing and 3D structural modelling: in Hill, K.C., and Bernecker, T. (eds), *Eastern Australasian Basins Symposium: a refocused energy perspective for the future*: Petroleum Exploration Society of Australia, 373–384.

Root, R.S., Gibson-Poole, C.M., Lang, S.C., Streit, J.E., Underschultz, J.R., and Ennis-King, J., 2004, Opportunities for geological storage of carbon dioxide in the offshore Gippsland Basin, SE Australia: an example from the upper Latrobe Group: in Boult, P.J., Johns, D.R., and Lang, S.C., (eds), *Eastern Australasian Basins Symposium II, Special Publication*: Petroleum Exploration Society of Australia, 367–388.

Santarelli, F.J., Tronvoll, J., Svennekjaer, M., Skele, H., Henriksen, R., and Bratli, R.K., 1998, Reservoir stress path: the depletion and the rebound. *SPE/ISRM Eurock 98 Conference, Trondheim, Norway*, **2**, 203–209. SPE 47350.

Shimamoto, T., and Logan, J.M., 1981, Effects of simulated clay gouge on the sliding behaviour of Tennessee sandstone: *Tectonophysics*, **75**, 243–255.

Sibson, R.H., 1974, Frictional constraints on thrust, wrench and normal faults: *Nature*, **249**, 542 – 544.

Sibson, R.H., 1996, Structural permeability of fluid-driven fault-fracture meshes: *Journal of Structural Geology*, **18**, 1031–1042.

Streit, J.E., and Hillis, R.R., 2004, Estimating fault stability and sustainable fluid pressures for underground storage of CO2 in porous rock: *Energy*, **29**, 1445–1456.

Tuefel, L.W., Rhett, D.W., and Farrell, H.E., 1991, Effect of reservoir depletion and pore pressure drawdown on in situ stress and rock deformation in the Ekofisk Field, North Sea: in Roegiers, J.C. (ed.), *Rock Mechanics as a Multidisciplinary Science*, Balkema, 63–72.

Wiprut, D., and Zoback, M.D., 2000, Fault reactivation and fluid flow along a previously dormant normal fault in the northern North Sea: *Geology*, **28**, 595–598.

オーストラリアGippsland BasinにおけるCO_2圧入中の断層再活性化の可能性

ピーター J. バン＝ルース[1]・エマ J. ネルソン[1]・リチャード R. ヒリス[1]

要　旨：　現在の圧力場中で、断層再活性化を誘起するのに必要な孔隙圧増加を見積もって、断層再活性化の危険を決定するFAST(Fault Analysis Seal Technology)という手法を使って、Gippsland Basinの断層再活性化の危険性を計算した。Gippsland Basinの応力場は横ずれ断層帯と逆断層帯の境界にあり、最大水平応力(~40.5MPa/km) >垂直応力(21MPa/km)の~最小水平応力(20MPa/km)である。孔隙圧はGolden BeachSubgroupのCampanian期火成岩以浅では静水圧程度である。ここで決定された北西-南東(139°N)方向の最大水平応力は、予想された主応力方向とおおむね一致し、Gippsland Basinの最大水平応力の方向が北西-南東であることが確認された。Gippsland Basinの断層の再活性化の危険性はcohesionless断層(C = 0; μ = 0.65)とhealed断層(C=5.4; μ=0.78)の2つの断層強度のシナリオを想定して計算された;。healed断層とcohesionless断層どちらのシナリオを用いても、再活性化可能性の比較的高い断層も低い断層いずれも、その走向はほぼ一致した。北西-南東の走向をもつ高傾斜断層は現在の応力場では再活性化の可能性は低い。南南東―北北西および東北東―西南西の走向を持つ高傾斜断層は、断層再活性化の危険性が最も高い。また、走向NE-SWの低傾斜断層(逆断層)にも比較的高い再活性化リスクがある。再活性化リスクの最も高い走向を持った断層の孔隙圧上昇(ΔP)は、cohesionless断層の場合3.8MPa(~548psi)、healed断層の場合は15.6MPaと推測される。

この論文に提示された断層再活性化分析から、得られた孔隙圧上昇の絶対値には地質工学的モデル(現位置での応力場と岩石強度)の不確定性による大きな誤差が含まれている事が予想される。特に、最大水平応力の値と断層強度データは十分に制御されていない。したがって、断層再活性化分析を貯留層中で許容できる最大孔隙孔圧上昇の直接測定に使用することはできない。筆者らは、この種の断層再活性化分析は断層再活性化の危険を相対的に評価するといった目的にのみに限定して使用すべきで、再活性化するまでに断層が耐えられる最大孔隙圧上昇の許容限界の決定、といった目的でこの手法を使用すべきでないと結論する。

キーワード：断層再活性化、CO_2圧入、地質工学的危険度

호주 Gippsland Basin에서 CO_2 주입 중 단층 재활성화의 가능성

Peter J. van Ruth[1], Emma J. Nelson[1], and Richard R. Hills[1]

요　약：　현재의 응력장내에서 단층 재활성화를 야기하는데 필요한 공극압의 증가를 추정함으로써 재활성화 위험도를 결정하는 FAST(단층 분석 확인 기술)를 이용해 Gippsland Basin의 단층 재활성의 위험도가 계산되었다. Gippsland Basin의 응력 형태는 주향이동단층과 역단층의 경계부근으로서 즉, 최대 수평 압력(~40.5 MPa/km) > 수직 압력(21 MPa/km) ~ 최소 수평 압력(200 MPa/km)이다. 공극압은 Golden Beach Subgroup의 Campanian Volcanics 상부에서 정수압이다. 여기에서 결정된 NW-SE 최대 수평 응력 방향(139 °N)은 이전의 측정값들과 대체로 일치하고 Gippsland Basin 에서의 NW-SE 최대 수평 응력 방향을 입증한다. Gippsland Basin의 단층 재활성화 위험도는, cohesionless fault(C=0; μ=0.65)와 healed fault(C=5.4; μ=0.78), 두 가지 단층 강도 시나리오를 이용해서 계산되었다. 상대적으로 높고 낮은 재활성화 가능성을 가진 단층들의 방향은 cohesionless fault 와 healed fault 모두에 대해 거의 동일하다. NE-SW 주향방향의 큰 각을 가진 단층들은 현재의 응력상태하에서는 재활성화 가능성이 거의 없다. SSE-NNW 과 ENE-WSW 방향의 큰 각을 가진 단층들이 단층 재활성화 위험도가 가장 높다. 부가적으로 NE-SW 주향 방향의 작은 각을 가진 단층(thrust 단층)은 상대적으로 높은 재활성화 위험도를 가지고 있다. 최적 방향 단층들에 대한 가장 높은 재활성화 위험도는 cohesionless fault 에 대해서는 추정 공극압의 3.8MPa(~548psi) 증가(Delta P), healed fault 에 대해서는 15.6MPa 증가에 해당된다. 이 논문에서 제시된 단층 재활성화 분석으로부터 얻은 공극압 증가의 절대값은 지구역학적인 모델(원위치 응력과 암석 강도 자료)에서의 불확실성으로 인해 큰 오차를 수반한다. 특히, 최대 수평 응력 강도와 단층 강도 자료는 좁은 범위에 한정되어 있지 않다. 그러므로 단층 재활성화 분석은 저류층 내에서 최대로 허용할 수 있는 공극압 증가를 직접 측정하는데 사용될 수 없다. 이러한 종류의 단층 재활성화 분석은 단지 단층 재활성화의 상대적인 위험도의 평가에 사용될 수 있을 뿐이고, 재활성화에 앞서 단층이 견딜 수 있는 공극압 증가의 최대 허용치를 결정하는데는 사용할 수 없다고 주장하고자 한다.

주요어：단층 재활성화, CO_2 주입, 지구역학적 위험도

温暖化ガス技術共同研究センター
1 アデレード大学　石油学部
North Terrace, ADELAIDE, SA, Australia 5000

Cooperative Research Centre for Greenhouse Gas Technologies
1 Australian School of Petroleum, The University of Adelaide